Journal of the Ceramic Society of Japan 117 [7] 851-855 2009 **Express letter**

SnO_2-based varistors capable of withstanding surge current

Zhen-ya LU,† Zhiwu CHEN and Jian-qing WU

Key Lab of Special Functional Materials of Ministry of Education, College of Materials Science & Engineering, South China University of Technology, Guangzhou 510640, China

SnO_2-based varistor material was fabricated by doping of CoO, Nb_2O_5, Cr_2O_3, and Y_2O_3 or Ho_2O_3. The microstructure, nonlinear *I–V* characteristic and surge current performances have been investigated. The average grain boundary voltage of the obtained materials is close to that of ZnO varistors. Similar to Cr^{3+}, Y^{3+} or Ho^{3+} acts as the acceptor in the grain boundaries and the depletion layers. Moderate co-doping Y_2O_3 or Ho_2O_3 with Cr_2O_3 is helpful to improve the electrical performances and to prevent poor densification. The obtained optimal samples with a diameter of about 14 mm have a nonlinear coefficient (α) of about 60, threshold electric field (E_b) of about 380 V/mm, and the withstanding peak current of 8/20 μs wave is about 2400 A. Higher surge current will cause failure but no visual damage happen. This kind of failure mode is helpful for safety use of varistors.

Key-words : SnO_2, Varistor, Y_2O_3, Ho_2O_3, Nonlinear, Surge current test, Failure mode

[Received February 12, 2009; Accepted May 21, 2009]

1. Introduction

With the unique nonlinear characteristics and high energy handling capability, ZnO-based varistors are widely used both in electric power distribution networks as well as electronic circuits to absorb or to suppress transient voltage surges and to do so repeatedly without being destroyed.[1] Many researchers worked at the mechanism or theory of ZnO-based varistors from 1970's to 1990's. The transient voltage suppressing capability of commercial MOV products had been improved rapidly in those years. In recent years, although research papers on manufacturing process[2)–3)] and on fundamental theories[4)–5)] of ZnO-based varistor material were still published frequently, no significant progress was made recently on the electrical properties. So, research work on different varistor materials is worthwhile.

SnO_2-based varistor was reported quite long ago. But it still can't be technically used. SnO_2–Bi_2O_3–Co_3O_4–BaO–Nb_2O_5 varistor with nonlinearity coefficient of 20 was prepared in 1989,[6] and SnO_2–CoO–Nb_2O_5–Cr_2O_3 varistor with nonlinearity coefficient of 41 was reported in 1995.[7] Many research articles on SnO_2-based varistor materials are published in the past ten years. Much attention has been focused on the Schottky-type potential barriers.[8)–10)]

In literature, SnO_2-based varistor materials with nonlinear coefficient comparable to the commercial ZnO varistor materials have been reported. Different oxides were introduced to SnO_2-based materials to improve the densification and nonlinearity. CoO is an effective dopant to achieve highly densified SnO_2 ceramics.[7] It was reported that doping Cr_2O_3 could increase the nonlinear coefficient α of the SnO_2–CoO–Nb_2O_5 system to be 41,[7),11)] or even to be 75.[12] La_2O_3, Pr_2O_3, CeO_2, Yb_2O_3, and Bi_2O_3 were also reported to be good additives for nonlinearity.[13)–17)] However, most of these nonlinear facilitating additives will result in increasing of the threshold electric field and decreasing of the ceramic density.[13)–15)]

The crystalline phases of SnO_2-based varistor ceramics doped with different additives have been investigated by means of XRD analysis in some published papers.[7),11),14),15)] No other phase was found except for cassiterite with rutile crystalline structure.

The nonlinear coefficient α is generally tested in low DC current region, such as 0.1 to 1.0 mA or 1.0 to 10.0 mA. High α value does not imply good performance in high current region. For a varistor to be used to protect electric or electronic circuits against transient voltage surges induced by lightning or switching, high α value is basically required, but more importantly, it should be capable of withstanding surge current. Therefore, to investigate the high current performance is an essential work for developing applicable SnO_2-based varistor materials. Recently, Ramirez et al. reported the degradation behavior of SnO_2-based varistors due to current pulses.[18]

Up to now, SnO_2-based varistor materials with surge current performances comparable to the widely used ZnO-based varistor materials have not been reported.

In this paper we present our research results mainly on the surge current performances of SnO_2-based varistor materials. And the failure mode was investigated due to surge current test.

2. Experimental procedure

Samples were prepared by conventional electroceramic processes. The composition in molar ratio of the investigated systems is listed in **Table 1**.

SnO_2 powder (purity of 99.5%) was blended with additives and ball milled with distilled water. PVA solution was used as the binder for granulation process. The granulated powder was

Table 1. Compositions of Samples

Sample	SnO_2	CoO	Nb_2O_5	Cr_2O_3	Y_2O_3	Ho_2O_3	Reference
SCNCr–1	98.9	1.0	0.05	0.05			7
SCNCr–2	97.4	2.5	0.05	0.05			This work
SCNCrY	97.37	2.5	0.05	0.05	0.05		This work
SCNCrHo	97.37	2.5	0.05	0.05		0.05	This work

† Corresponding author: Z. Lu; E-mail: zhylu@scut.edu.cn

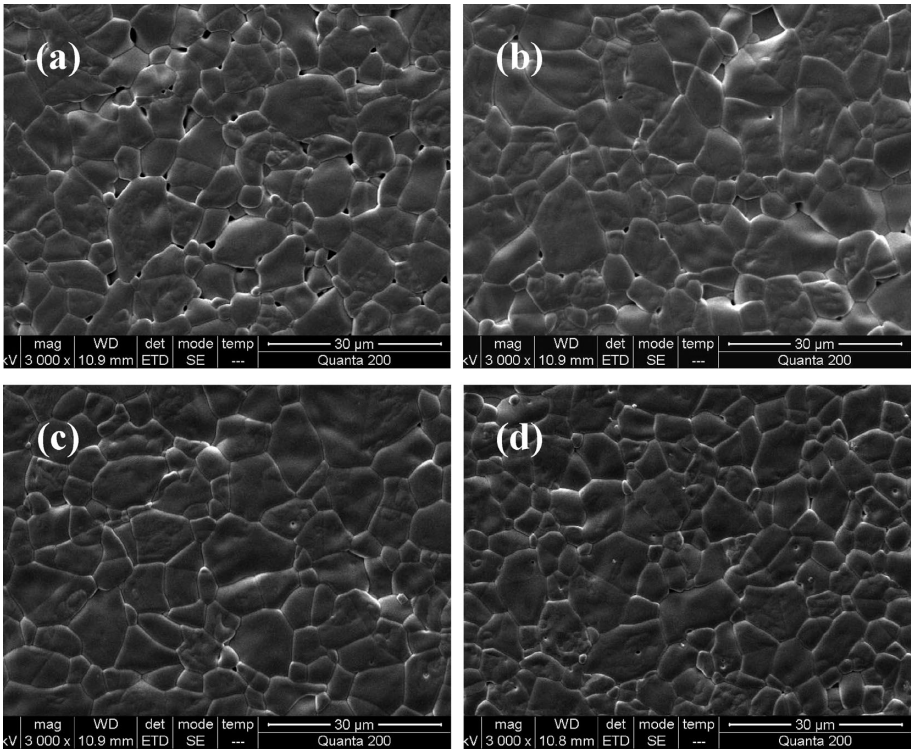

Fig. 1. SEM micrographs of the sintered samples. The samples were polished and thermally etched at 1250°C for 20 min to reveal the grain boundaries. (a) sample SCNCr–1, (b) sample SCNCr–2, (c) sample SCNCrY and (d) sample SCNCrHo.

pressed into discs at a pressure of about 150 MPa. After burned out the organic binder, the discs were placed in a covered aluminum crucible and sintered at 1300°C for 2 h in air. Black ceramic discs with a diameter of about 14 mm and a thickness of about 1.0 mm were obtained. The sintered discs were annealed at 750°C for 2 h. Electrodes were made on both surfaces of the black discs with silver paste printing and firing at 600°C. The resulting varistor discs can be used for measurement of low current parameters, including varistor voltage V_{1mA}, nonlinear coefficient and leakage current. The threshold electric field E_b is calculated from V_{1mA} and the thickness of the tested sample. For surge current testing, the discs with electrodes were soldered with tinned copper terminals and coated with epoxy resin.

The densities of the sintered samples were determined by the Archimedes methods. Considering the small volume proportion of the additives and the unchanged crystalline main phase, the theoretical density of the specimens was supposed to be 6.95 g/cm^3, which is the theoretical density of SnO_2. Microstructure characterization of sintered samples was made by scanning electron microscope (SEM; FEI–Quanta 200). The polished surface was thermally etched at 1250°C for 20 min to reveal the grain boundaries. The crystalline phases of the sintered samples were analyzed by means of X-ray diffraction (XRD) with Philips X'pert MPD. The sintered samples for XRD analysis were pulverized.

3. Results and discussion

Figure 1 shows SEM micrographs of the sintered samples. These micrographs show clearly that the porosity in sample SCNCr–1 is much higher than that in SCNCr–2, SCNCrY and SCNCrHo. CoO is a crucial additive for SnO_2-based varistor. It can improve the densification of SnO_2-based varistor system.[7] Higher concentration of CoO in sample SCNCr–2, SCNCrY and SCNCrHo has further improved the densification.

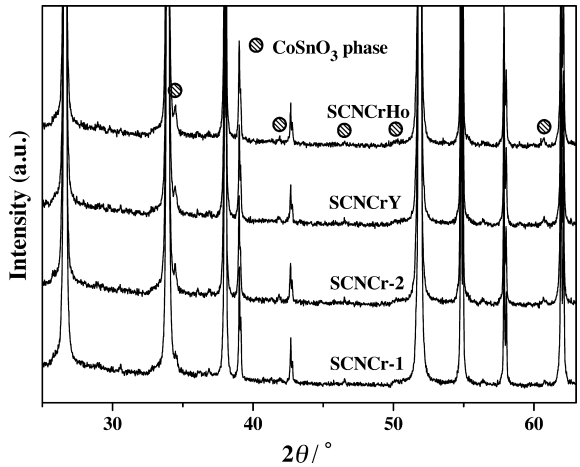

Fig. 2. XRD patterns for all sintered samples. The filled circles indicate the peaks positions of the $CoSnO_3$ phase.

It is difficult to identify secondary phase grains in the micrographs in Fig. 1. However, X-ray diffraction patterns shown in **Fig. 2** reveals that, besides diffraction peaks of the main phase SnO_2, the diffraction peaks of $CoSnO_3$ phase (JCPDS PDF 28–1236) were also found in all the samples. The diffraction peaks of $CoSnO_3$ phase were intensified in the XRD patterns of sample SCNCr–2, SCNCrY and SCNCrHo by increasing the concentration of CoO.

The doping element Co was considered to form a solid solution by means of the substitution of Sn^{4+} ions by Co^{2+} or Co^{3+} ions.[7] For one-to-one substitution, the lower valent Co^{2+} or Co^{3+} ions acting as acceptors should compensate the effect of the donor dopant Nb_2O_5. The substitution should happen only in the

Table 2. Relative Density, Mean Gain Size and Electrical Performance

System	Relative density (%)	Mean grain size (μm)	E_b (V/mm)	Barrier voltage V_{gb}	Nonlinear coefficient α	Residual voltage ratio V_{500A}/V_{1mA}	withstanding peak current (A)**
SCNCr–1	96.26	5.4	415	2.24	50	2.55	600
SCNCr–2	97.55	7.0	310	2.17	56	2.51	1500
SCNCrY	97.27	6.4	363	2.32	60	2.15	2400
SCNCrHo	97.10	6.2	385	2.39	55	2.20	2000
ZnO varistor*	/	/	218	/	61	1.69	6500

*commercial ZnO based varistor sample, the dimension of the ceramic disc is about ϕ14 × 1.82, the varistor voltage (V_{1mA}) before surge test is 397 V.
**The peak value of the surge current with a standard 8/20 μs waveform.

grain boundary layer otherwise the sintered samples can not be varistor materials. According to the aforesaid XRD analysis results, it is reasonable to deduce that most of the added CoO reacts with SnO_2 to form a secondary phase $CoSnO_3$.

The mean crystal grain sizes listed in **Table 2** were determined by the intercept method.[19] According to the mean grain sizes and the threshold electric field E_b listed in Table 2, the single grain boundary voltage or barrier voltage (V_{gb}) of the tested samples can be estimated to be about 2.1~2.4 V, which is close to the barrier voltage of ZnO varistors.[1]

As shown in Table 2, the measured nonlinear coefficient, which is defined as $\alpha = 1/\log (V_{1mA}/V_{0.1mA})$, of all the listed obtained samples are good enough for application and are comparable with that of the commercial ZnO base varistor sample shown in the same table.

To test their surge current performances, samples were subjected to 8/20 μs waveform current impulses. The standard 8/20 μs waveform current impulse (refer to the standard: IEC 61643–1–2005) has been widely used for surge current test of varistors or surge protective devices (SPDs). An 8/20 μs wave surge current generator was used for the test. The surge current waveform and the response voltage waveform are recorded simultaneously using an oscilloscope (Rigol DS 1062). Varistor voltage at DC current 1 mA was measured before and after the surge current test. The withstanding peak current listed in Table 2 is defined as the maximum peak value of the recorded current wave, after being subjected to this surge current, without visual damage happen to the tested sample and the change of varistor voltage V_{1mA} is smaller than ±10%. For comparison, commercial ZnO base varistor samples with comparative diameters and varistor voltages (see Table 2) was also tested in the same way.

As shown in Table 1 and Table 2, when the CoO concentration increases from 1.0 mol% (system SCNCr–1) to 2.5 mol% (system SCNCr–2), the surge current performance is improved greatly. Higher concentration of CoO lowered the porosity (see Fig. 1) and may further improve the grain boundary structure, the number of the active nonlinear grain boundaries[20] increases, the surge current performance can be improved consequently.

A small quantity of the rare earth addition Y_2O_3 (system SCNCrY) or Ho_2O_3 (system SCNCrHo) is much helpful for the surge current withstanding capability (see Table 2). Similar to Cr^{3+}, Y^{3+} or Ho^{3+} acts as the acceptor in the grain boundaries and the depletion layers. Higher concentration of Cr_2O_3 is harmful to the densification and electrical performances.[11] However, we found moderate co-doping Y_2O_3 or Ho_2O_3 with Cr_2O_3 is helpful. The acceptor Cr^{3+} and Y^{3+} or Ho^{3+} should distribute in different location for their difference of the ion radii, the smaller cation

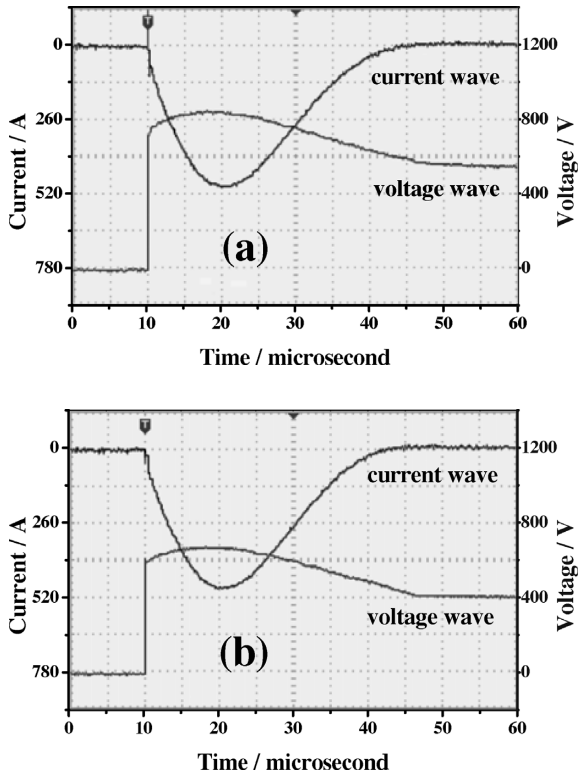

Fig. 3. Surge current wave and response voltage wave. (a) sample of System SCNCrY, the residual voltage peak is about 845 V, and the varistor voltage V_{1mA} = 392 V, (b) ZnO varistor sample, the residual voltage peak is about 670 V, and the varistor voltage V_{1mA} = 397 V. The current peak for both (a) and (b) is about 500 A. The voltage wave didn't fall to zero, that resulted from the underdamped state of the surge discharge circuit and the capacitive effect of the samples.

Cr^{3+} get deeper to the depletion layer. Co-doping Y_2O_3 or Ho_2O_3 with Cr_2O_3 make the depletion layer to be thicker and stronger to withstand the surge current.

Figure 3 shows the recorded current wave and voltage wave for surge current testing of sample SCNCrY and the comparative ZnO varistor sample. The voltage responses of them to the 8/20 μs waveform surge current are similar except for the different residual voltage, which is defined as the peak value of the voltage wave responding to a given surge current wave (refer to the standard: IEC 61643–1–2005).

The residual voltage is a crucial parameter for a surge protective device. The residual voltage ratio listed in Table 2 is defined

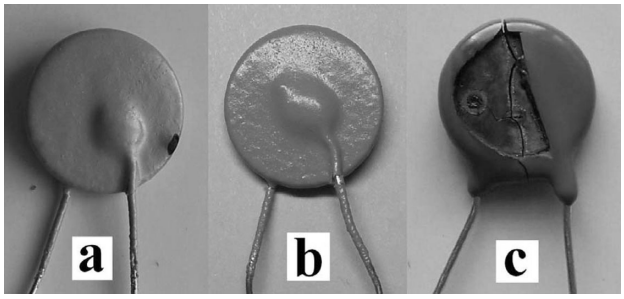

Fig. 4. Failed samples after high surge current test. (a) Sample SCNCr–1 after a surge current with a peak of 1500 A, (b) Sample SCNCrY after a surge current with a peak of 4000 A and (c) ZnO varistor sample after a surge current with a peak of 8500 A.

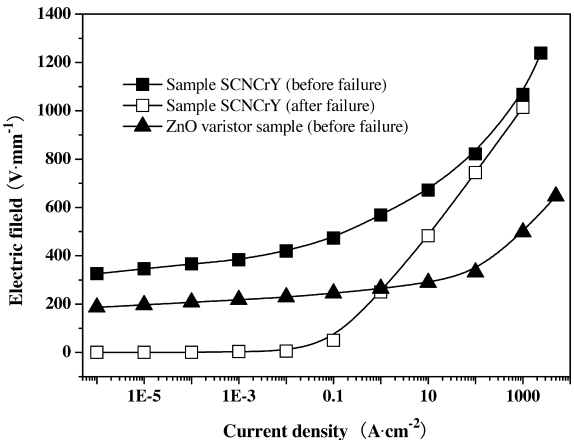

Fig. 5. *J–E* characteristic of sample SCNCrY and the comparative ZnO varistor. After failure, serious degradation happened in low current region of the *J–E* curve of sample SCNCrY.

as the ratio of the residual voltage to the sample's varistor voltage V_{1mA} when the surge current peak is about 500 A. As shown in Fig. 3, to a surge current with about 500 A peak value, the voltage responses of the obtained SCNCrY sample and the comparative ZnO varistor sample are similar in shape, but the residual voltage of system SCNCrY is higher than that of ZnO varistor sample although their varistor voltage V_{1mA} are nearly equivalent. The calculated residual voltage ratios are 2.15 and 1.69 respectively (see Table 2).

The lower residual voltage ratio means the better limiting voltage performance. The limiting voltage performance of the obtained SnO_2-base varistor should be further improved.

Comparing to the ZnO varistor sample, the withstanding surge current of the obtained SnO_2-based varistor samples is smaller (see Table 2). However, considering the difference of the threshold electric field E_b and the residual voltage ratio, the absorbing surge energy density E_v of the obtained sample SCNCrY is comparable to that of the tested ZnO varistor sample, according to Eq. (1).

$$E_v = \frac{1}{v}\int I(t)\cdot V(t)\mathrm{d}t \qquad (1)$$

where v is volume of the ceramic disc of the tested sample.

If the residual voltage ratio can be lowered further by composition optimizing or new manufacture process, the withstanding surge current of the SnO_2-based varistor will increase correspondingly.

Cracking and puncture are typical failure modes of ZnO varistors due to surge current.[21] However in this work, for most of the failure samples after surge current test, no cracking or puncture happen. Practically, no visual destruction happen to most of the failure samples except for some samples of system SCNCr–1. Side flashover traces were observed in some failure samples of system SCNCr–1. We ascribe this failure to the higher threshold electric field E_b. It was found that the epoxy insulating coat is not good enough to prevent the flashover when the threshold electric field E_b is higher than 400 V/mm. When side flashover happened, the surge current flowed through the side flashover traces instead of the bulk varistor material, and no puncture or cracking happened.

Figure 4 shows the pictures of the failed samples after surge current test. A side flashover trace can be seen on the failed sample SCNCr–1 (see Fig. 4(a)).

For most of the tested samples of system SCNCr–2, SCNCrY and SCNCrHo, when the surge current peak is higher than the withstanding peak current listed in Table 2, the current-voltage characteristic degraded severely. The varistor voltage V_{1mA} of some failed samples decreased nearly to be zero although without visual damage happen (see Fig. 4(b)).

As for the comparative ZnO samples, the failure mode is different, after subjected to a surge current with a peak of 8500 A, the sample cracked (see Fig. 4(c)), that is consistent with the result of Eda.[21]

The different failure modes between sample SCNCrY and the comparative ZnO varistor should be related to the different thermal conductivity. Bueno et al. reported the SnO_2-based varistor system showed a thermal conductivity higher than that of ZnO-based varistors.[22] When surge energy was injected into the tested specimens, higher thermal conductivity could improve the temperature uniformity of the ceramic materials and reduce the probability of the thermal-mechanical failure.

Figure 5 shows the *J–E* characteristic of a SCNCrY sample. Before failure, the nonlinear performance is similar to that of a commercial ZnO varistor. The failure sample SCNCrY behaves as a several kΩ resistor in low current region, but in higher current region, the *J–E* curve tends to be close to that of a normal sample (before failure). The voltage response to higher current may be come from the undamaged grain boundary barriers. While the linked damaged grain boundary barriers serves as the current pathway in the low current region.

4. Conclusions

In summary, SnO_2-based varistor materials with promising surge current performance were fabricated. CoO is a crucial dopant for the investigated SnO_2-based varistor. Higher concentration of CoO further enhances the density and may improve the grain boundary structure, the surge current performance can be improved consequently. Co-doping Y_2O_3 or Ho_2O_3 with Cr_2O_3 make the depletion layer to be thicker and stronger to withstand the surge current. The failure mode of the obtained SnO_2-based varistor is different from that of the comparative commercial ZnO-based varistor samples. Further works is needed to lower the residual voltage ratio and to further improve the surge current performances of the investigated SnO_2-based varistors.

Acknowledgement This work is funded by the Scientific and Technological Planning Project of Guangdong Province (No. 2006A11003001) and by the Scientific and Technological Planning Project of Guanghou City (No. 2006Z3–D0431).

References

1) T. K. Gupta, *J. Am. Ceram. Soc.*, 73, 1817–1840 (1990).
2) S. Hirose, K. Nishita and H. Niimi, *J. Appl. Phys.*, 100, 083706 (2006).
3) Y. K. Li, G. R. Li and Q. R. Yin, *Mater. Sci. and Eng. B*, 130, 264–268 (2006).
4) D. Fernández-Hevia, J. de Frutos, A. C. Caballero and J. F. Fernándezb, *J. Appl. Phys.*, 92, 2890–2898 (2002).
5) M. Elfwing and E. Olsson, *J. Appl. Phys.*, 92, 5272–5280 (2002).
6) A. B. Glot and A. P. Zlobin, *Inorganic Mater.*, 25, 274–276 (1989).
7) S. A. Pianaro, P. R. Bueno, E. Longo and J. A. Varela, *J. Mater. Sci. Lett.*, 14, 692–694 (1995).
8) P. R. Bueno, S. A. Pianaro, E. C. Pereira, L. O. S. Bulhoes, E. Longo and J. A. Varela, *J. Appl. Phys.*, 84, 3700–3705 (1998).
9) P. R. Bueno, M. R. de Cassia-Santos, E. R. Leite, E. Longo, J. Bisquert, G. Garcia-Belmonte and F. Fabregat-Santiago, *J. Appl. Phys.*, 88, 6545–6548 (2000).
10) P. R. Bueno, E. R. Leite, M. M. Oliveira, M. O. Orlandi and E. Longo, *Appl. Phys. Lett.*, 79, 48–50 (2001).
11) S. A. Pianaro, P. R. Buenob, E. Longob and J. A. Varela, *Ceramic International*, 25, 1–6 (1999).
12) J. S. Vasconcelos, N. S. L. S. Vasconcelos, M. O. Orlandia, P. R. Bueno, J. A. Varela, E. Longo, C. M. Barrado and E. R. Leite, *Appl. Phys. Lett.*, 89, 152102 (2006).
13) P. R. Bueno, M. M. Oliveira, W. K. Bacelar-Junior, E. R. Leite and E. Longo, *J. Appl. Phys.*, 91, 6007–6014 (2002).
14) M. M. Oliveira, P. R. Bueno, M. R. Cassia-Santos, E. Longo and J. A. Varela, *J. Eur. Ceram. Soc.*, 21, 1179–1185 (2001).
15) M. M. Oliveira, P. R. Buenoa, E. Longoa and J. A. Varela, *Mater. Chem. Phys.*, 74, 150–153 (2002).
16) P. Qi, J. F. Wang, W. B. Su, H. C. Chen, G. Z. Zang, C. M. Wang and B. Q. Ming, *Mater. Sci. Eng. B*, 119, 94–98 (2005).
17) I. Skuratovsky, A. Glot, E. Di Bartolomeo, E. Traversa and R. Polini, *J. Eur. Ceram. Soc.*, 24, 2597–2604 (2004).
18) M. A. Ramirez, W. Bassi, P. R. Bueno, E. Longo and J. A. Varela, *J. Phys. D: Appl. Phys.*, 41, 122002 (2008).
19) M. I. Medelson, *J. Am. Ceram. Soc.*, 52, 443–446 (1969).
20) M. Bartkowiak, G. D. Mahan, F. A. Modine and M. A. Alim, *J. Appl. Phys.*, 79, 273–281 (1996).
21) K. Eda, *J. Appl. Phys.*, 56, 2948–2955 (1984).
22) P. R. Bueno, J. A. Varela, C. M. Barrado, E. Longo and E. R. Leite, *J. Am. Ceram. Soc.*, 88, 2629–2631 (2005).